American Mineralogist, Volume 76, pages 880–891, 1991

Thermodynamic properties of pyrope and grossular from vibrational spectroscopy

A. M. Hofmeister
Department of Geology, University of California, Davis, California 95616, U.S.A.
A. Chopelas
Max-Planck-Institut für Chemie, D 6500, Mainz, Germany

Abstract

Heat capacity C_V and entropy S for pyrope and grossular are calculated using a statistical thermodynamic approach and a density of states derived from previous single-crystal infrared and Raman spectra obtained for natural, nearly end-member garnets. Calculations of C_P agree with calorimetric data from ~150 to ~1000 K, within 0.6% for pyrope and within 1% for grossular. Results for S parallel the calorimetric values but are offset by propagation of the heat capacity mismatch at low temperatures, through the integration of C_P/T over temperature. Calculated S for pyrope is offset by about −10 J/mol K, and S of grossular is offset by +8 J/mol K. Calorimetric data at low temperatures (50–150 K) are outside the limit of uncertainty in spectroscopic derivation, possibly because of positional disorder of Mg in pyrope or replacement of SiO_4 by 4OH in grossular, or both. This conclusion is supported by comparison of relative entropies, in that the theory predicts that the entropy of pyrope is less than that of grossular, whereas calorimetric measurements yielded the opposite result. Preferred values of thermodynamic properties in J/mol K at 298.15 K are C_P(Py) = 326.0 ± 0.5, S(Py) = 256 ± 1, C_P(Gr) = 333.5 ± 0.5, and S(Gr) = 265 ± 2. Excess entropy of grossular compared to pyrope results from the larger mass of the Ca ion; however, its magnitude is limited by the large size of the Ca ion, which dilates the Si-O bond through edge sharing of the larger dodecahedra with the tetrahedra, leading to changes in the force constants that raise the frequency of the lowest lying translations of the SiO_4 tetrahedron. This type of compositional dependence of bonding is inferred to regulate mixing properties of garnets.

Introduction

The ubiquitous occurrence of garnets in igneous, metamorphic, and upper mantle rocks, coupled with their involvement in reactions that are useful primarily as geobarometers, mandates thorough and accurate knowledge of the thermodynamic properties of these minerals. Although the body of data precisely delineating equilibrium conditions for reactions involving garnet and providing increasingly accurate physical measurements of end-members and solid solutions has expanded considerably over the last decade (e.g., Koziol and Newton, 1988; Haselton and Westrum, 1980), numerous questions and problems exist (see for example, the discussion by Hodges and McKenna, 1987). In particular, information on mixing properties is essential because natural garnets are usually multicomponent; yet phase equilibria are generally determined for end-member garnets and departures from ideality are expected because of large size differences between the cations substituting in the same site in many garnet solid solutions (e.g., Mg^{2+} and Ca^{2+}).

A number of attempts have been made to estimate mixing data. Most recently, mixing properties of aluminous garnets derived from phase equilibria have been shown to be inconsistent with mixing properties derived from their thermodynamic properties, suggesting that revisions are needed for both heat capacity and volume measurements (Berman, 1990). Sigmoidal curvature previously derived for variation in mixing volumes (Newton and Wood, 1980 and references therein) is not supported by Berman's (1990) model; on the other hand, microscopic changes in pyrope-grossular and almandine-grossular solid solutions derived from analysis of vibrational spectra from these binary systems indicate that negative excess volumes may be possible near the small cation end-member (Hofmeister and Chopelas, 1991). Moreover, there is a problem in comparing different measurements for various garnets because symmetry may be dependent on conditions of formation (i.e., synthetic quenched samples vs. natural slowly cooled samples). Lastly, C_P data for Mg-Ca garnets are suspect because not only does the entropy of pyrope exceed that of grossular at low temperatures, contradicting expectations based on cation size and mass considerations, but also there is disagreement among various data sets for grossular (Haselton and Westrum, 1980; Westrum et al., 1979; Krupka et al., 1979; Kolesnik et al., 1979). In this paper, we are able to address the crucial, first-order problem concerning the accuracy of thermodynamic data for Mg-Ca garnets because the calorimetric measurements on these two

0003–004X/91/0506–0880$02.00

end-members can now be independently evaluated by calculation of their thermodynamic properties using information from single-crystal vibrational spectra in a Kieffer-type model.

Kieffer (1979, 1980) has developed a model based on lattice dynamics that allows calculation of heat capacity (C_V), entropy (S), and the Helmholz free energy (F) from vibrational frequencies and acoustic velocities. Calculated C_V can be compared to calorimetric measurements of C_P by using the anharmonic correction of

$$C_P = C_V + TV\alpha^2K_T \tag{1}$$

where K_T is the bulk modulus, V is volume, and α is the thermal expansivity. If IR and Raman data for polycrystalline samples are used to construct a simple density of states, heat capacities C_V are calculated to within 5% of the calorimetric results at 298 K and 1% at 700 K, but with large errors below 200 K. However, if band assignments based on accurate single-crystal infrared and Raman data are used to construct a detailed density of states, the accuracy is considerably improved (Hofmeister, 1987; Chopelas, 1990). It is critical to assess the accuracy below 200 K, since errors at low temperature propagate upward in T through the integral relating S to C_P. The accuracy is largely dependent on the quality of the data, the validity of the band assignments, and the range and distribution of the vibrational modes, especially for those below 200 cm^{-1} (Hofmeister et al., 1987; Hofmeister and Ito, in preparation). A higher degree of accuracy is expected for garnet, because it not only has an unusually large number of modes over the large frequency interval typical of silicates, but it also has well-established band assignments based on completely known zone-center vibrational spectra (Hofmeister and Chopelas, 1991).

In this paper, we show that heat capacity and entropy of pyrope and grossular can be calculated to better than $\pm 1\%$ using a density of states constructed from single-crystal spectroscopic data. The calculated values are sufficiently accurate that detailed comparisons between calculated and measured heat capacities yield some insight into reasons for discrepancies among the various measurements. This, in turn, suggests which data are representative of thermodynamic parameters for these garnets over a large temperature range. Ramifications for phase equilibria and petrological applications are discussed. The microscopic basis for the entropy of grossular exceeding that of pyrope at 298 K is discussed and explanations for the contradictory observations are explored.

Vibrational modeling

The thermodynamic functions for a vibrating system can be calculated using a statistical approach where the energy levels of the system completely determine their values. The partition function Z represents a sum of factors corresponding to all possible energy levels of the system. A Boltzman distribution is used here. Thus, the statistical description of the heat capacity $C_V = (dE/dT)_V$ transforms from

$$C_V = \frac{k}{T^2}\frac{\partial^2 \ln Z}{\partial(1/T)^2} \tag{2}$$

to

$$C_V = k\int_0^{\nu_L} \frac{e^{h\nu/kT}}{(e^{h\nu/kT}-1)^2}\left(\frac{h\nu}{kT}\right)^2 g(\nu)\,d\nu \tag{3}$$

in a system of independent harmonic oscillators, where ν is the vibrational frequency, k is Boltzmann's constant, and h is Planck's constant (Reif, 1965; a complete set of equations is also given by Kieffer, 1979). Harmonic entropy is obtained by integrating

$$S_h = \int_0^T \frac{C_V}{T}\,dT. \tag{4}$$

Only two input values are required to determine a thermodynamic parameter: temperature T and the distribution of modes over frequency, known as the density of states $g(\nu)$. A model density of states $g(\nu)$ can be constructed from data derived from accurate vibrational spectral and elastic data using a modification of the method by Kieffer (1979), summarized here for completeness.

The primitive cell has $3N$ total degrees of freedom (where N is the number of atoms in the primitive cell). Three of these are the acoustic modes, which are determined from the acoustic velocities of the one compressional and the two shear waves. These modes are represented as Debye oscillators in the calculation by assuming that frequency varies sinusoidally with wavevector **k** (this variation is termed dispersion). The remaining $3N - 3$ degrees of freedom are the optic modes. Through the correlation method (Fateley et al., 1971) and factor group analysis (Farmer and Lazarev, 1974), the number of modes for each type of atomic motion in each symmetry category can be predicted. For orthosilicates such as garnet, the classifications include internal motions of the SiO_4 tetrahedron (asymmetric ν_3 and symmetric ν_1 Si-O stretching, asymmetric ν_4 and symmetric ν_2 O-Si-O bending), rotations and translations of the SiO_4 tetrahedron, and translations of the dodecahedral X and octahedral Y cations. These can be assigned to the various measured peaks in the spectra through systematic changes in frequency with chemical or isotopic substitution, or with physical parameters such as lattice constants, bond lengths, or atomic masses or both. For garnets in particular, band assignments were straightforward from the systematics in the vibrational data for five end-members where there is considerable variation in lattice parameters and a variety of cation sizes and masses (Hofmeister and Chopelas, 1991).

The distribution of modes over frequency (density of states) is assembled from the spectroscopic data as follows: high energy modes like ν_3 and ν_1 (or O-H stretching) that are clearly separable from the main body of vibrations are represented as Einstein oscillators. The similar-

TABLE 1. Vibrational model and input parameters for garnet

Type	Modes	Active	Total	Input frequencies (cm^{-1}) Pyrope	Grossular
Einstein 1	$T_{1u} + T_{2g}$ highest ν_3	6	10	1033	975
Einstein 2	E_g ν_3	2	6	938	904
Einstein 3	ν_1	3	12	918	866
Einstein 4	$T_{1u} + T_{2g}$ mid-low ν_3	12	20	890	848
Continuum 6	ν_4	20	36	667–510	631–505
Continuum 5	ν_2	11	24	562–439	549–416
Continuum 4	rotation (SiO_4)	15	36	400–350	406–349
Continuum 3	translation (Y)	9	24	478–279	474–245
Continuum 2	translation (X)	17	36	272–200	249–178
Continuum 1	translation (SiO_4)	17	33	342–140	330–159

Note: For the Einstein oscillators, the input frequencies are the average of the available Raman and IR data. For the continua, the input frequencies are the highest and the lowest of the observed modes in the category. All frequencies are from Hofmeister and Chopelas (1991).

ity of Raman T_{2g} to IR T_{1u} frequencies, as predicted from symmetry considerations, indicates that to a first approximation, we can predict frequencies of inactive modes from the existing data for each of the possible atomic motions. Thus, in garnets, the frequency of the doubly degenerate Raman E_g ν_3 mode is estimated to be similar to the average of frequencies of the inactive ν_3 modes in each of E_u, A_{1u}, and A_{2g}; the average frequencies of the measured two highest energy ν_3 triply degenerate Raman T_{2g} and IR T_{1u} bands are estimated to be similar to the average frequencies of four inactive modes within the T_{1g} and T_{2u} symmetries; and the average frequencies of the measured four lowest energy ν_3 triply degenerate T_{2g} and T_{1u} bands are estimated to be similar to the average frequencies of eight inactive modes within the T_{1g} and T_{2u} symmetries (Table 1). Each of the remaining atomic motions is represented as a separate continuum. (A complete symmetry analysis is given by Hofmeister and Chopelas, 1991). Upper and lower limits for the continua are taken as the upper and lower observed frequencies associated with the particular vibrational motion (Table 1). Thus, for ν_4, ν_2, R, and the translations, we are assuming that all inactive modes occur within the upper and lower limits of the observed modes.

Fewer continua can be used, but it has been our experience that greater accuracy is achieved with finer divisions of the optical modes (Hofmeister, 1987; Hofmeister et al., 1987; Chopelas, 1990; Hofmeister and Ito, in preparation). Selection of continua other than through factor group analysis involves a certain amount of arbitrariness in assembling a density of states, which in turn increases the uncertainty of the calculations.

Dispersion is not included, because it is essentially unknown (inelastic neutron scattering data on minerals are scant). Such neglect does not appear to measurably affect the results because dispersion can raise as well as lower frequencies. Ignoring dispersion is equivalent to averaging the three possibilities (frequency increases, decreases, or remains constant with wavevector **k**). For garnets and other materials with a large number of vibrational modes, this problem is further diminished because dispersion tends to be quite small (R. J. Hemley, personal communication, 1989). Furthermore, for cubic solids, the sum $\Sigma\nu_i^2(\mathbf{k})$ is a constant at any **k** (Hofmeister, in preparation), which shows that positive dispersion for some modes is offset by negative dispersion for others.

In summary, the density of states is assembled from a combination of three acoustic branches treated as Debye oscillators, several optic continua, and several Einstein oscillators. Data required for the model in addition to the infrared and Raman spectra (Table 1) are acoustic velocities derived from elasticity studies and unit-cell characteristics (Table 2). A few other thermodynamic parameters that are needed to relate theory to experiment using Equation 1 are listed in Table 2. The model for distribution of garnet modes with frequency is graphically depicted in Figure 1. The vibrational frequencies were obtained from natural, nearly end-member garnets. Vibrational frequencies of pyrope are spread out over a larger interval than those of grossular, and the positions of the highs and lows in the density of states differ slightly, but the overall shape and distribution of the modes are remarkably similar.

RESULTS AND COMPARISON WITH CALORIMETRY

Pyrope

The heat capacity C_P calculated for pyrope from Equations 1 and 3, using the density of states in Figure 1, reproduced the calorimetric data within its experimental uncertainty of +1% above 150 K (Table 3, Fig. 2). From 200 to 350 K, our calculated values are indistinguishable (<0.5% difference) from calorimetric data for synthetic pyrope of Haselton and Westrum (1980). Above 350 K, the calculated C_P is within 0.6% of the calorimetric values

TABLE 2. Parameters needed to calculate C_V and to compare it to C_P

Mineral	Formula	Volume* cm^3/mol	α** 10^{-6} K^{-1}	K_T† kbar	$V_P = U_3$ km/s	$V_s = U_{1,2}$ km/s	Density g/cm^3	dK_T/dT‡ kbar/K
Pyrope	$Mg_3Al_2Si_3O_{12}$	113.29	15.439 + 0.014T	1715	9.08	5.07	3.582	−0.258
Grossular	$Ca_3Al_2Si_3O_{12}$	125.30	14.288 + 0.013T	1675	9.34	5.05	3.594	−0.24

* Novak and Gibbs (1971).
** Least squares fit to data of Skinner (1966) by Kieffer (1980).
† Pyrope elasticity data from O'Neill et al. (1989); grossular from Bass (1989).
‡ From the compilation of Sumino and Anderson (1984); value for grossular was estimated from that measured for pyrope, almandine (−0.268), and spessartine (−0.22).

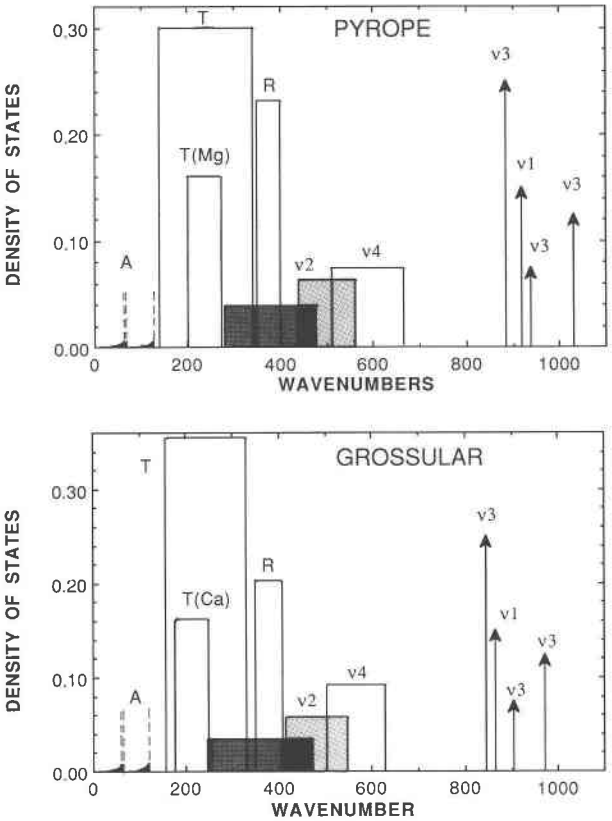

Fig. 1. Model density of states for pyrope (**top**) and grossular (**bottom**). The continua are represented as boxes with appropriate heights. The Einstein oscillators are represented as lines with heights proportional to the number of modes represented. Dotted lines represent the three acoustic modes. Labels indicate the band assignment for the modes involved (Table 1). Although the positions of the peaks and valleys in the density of states for pyrope differ somewhat from those of grossular, the overall shape and distribution are very similar.

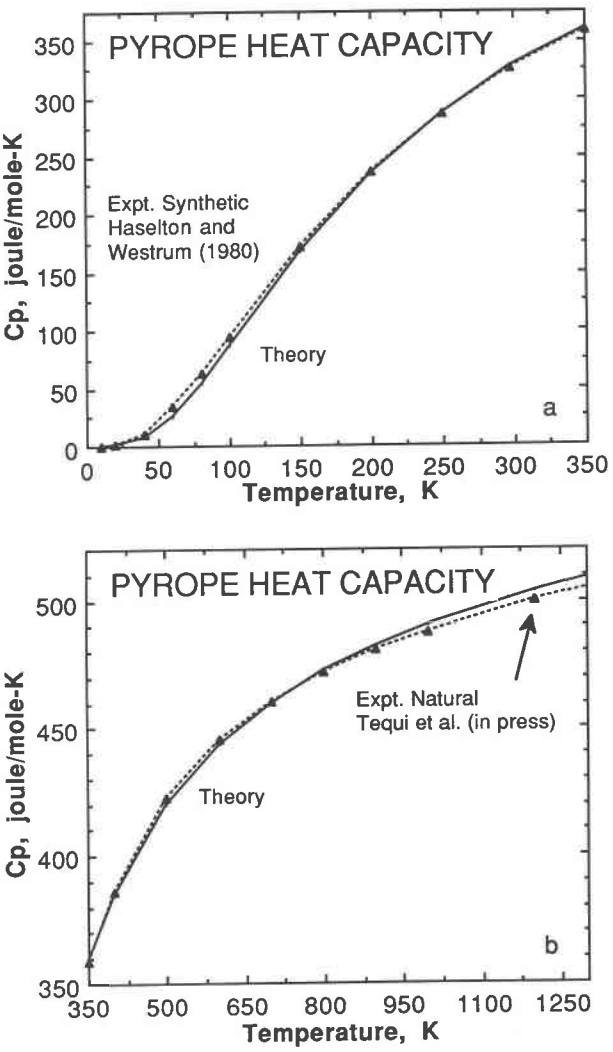

Fig. 2. Heat capacity of pyrope as a function of temperature. (**a**) Low temperature expansion. (**b**) High temperature results. (Note different scales for the C_P axis.) Solid line, C_P calculated from Kieffer's model using single-crystal vibrational frequencies measured from natural 94% pyrope. Dotted line with filled triangles, fit to calorimetric measurements on synthetic pyrope. Experiments below 350 K were conducted by Haselton and Westrum (1980); those above 350 K are from a fit to experimental data by Tequi et al. (1991) based on their drop calorimetric data from 750 to 1300 K and on DSC data from 350 to 650 K by Watanabe (1982).

of natural samples above 750 K (Tequi et al., 1991) and of synthetic samples from 400 to 750 K (Haselton and Westrum, 1980; Watanabe, 1982). However, between 10 and 200 K, the calculated values for pyrope lie slightly below the experiments, with a maximum departure of about 9 J/mol K at 80 K. It is possible that this discrepancy could be caused by some of the oscillators in the inactive symmetries having frequencies lower than the measured frequencies or by the lowest mode being dispersed to lower wavenumbers across the Brillouin zone. However, this is probably not the cause of the discrepancy because (1) the change in the distribution of oscillators as a result of including dispersion in order to produce a better match to the data from 0 to 200 K is likely to result in a poorer match at higher temperatures, and (2) dispersion is likely to be weak for solids with a large number of bands. Also, pyrope's frequencies are low considering that it contains only light cations. In fact, the lowest frequencies are comparable to those of garnets with much heavier cations (e.g., almandine and spessartine) because they originate as translations of SiO_4 groups, rather than of the dodecahedral cation. Therefore, inclusion of an arbitrary dispersion factor is not appropriate until calculated inactive modes are available either through lattice dynamics or from measurement of the spectra of an impure pyrope with lowered symmetry. Our spectroscopic model is the best possible theoretical representation of the density of states of pyrope at this time.

TABLE 3. Thermodynamic functions of pyrope

Temperature K	C_P theory J/mol K	C_P expt* J/mol K	C_P difference %	S theory J/mol K	S expt* J/mol K	S difference %
10.000	0.101	0.380	+73.5	0.034	0.013	−157.0
20.000	1.081	0.862	−25.4	0.411	0.197	−108.0
40.000	7.073	11.054	36.0	2.548	3.151	19.0
60.000	25.031	33.631	25.6	8.430	11.565	27.0
80.000	53.355	62.668	14.9	19.299	25.117	23.0
100.000	86.423	94.270	8.3	34.760	42.484	18.0
150.000	167.726	171.540	2.2	85.518	95.560	10.0
200.000	234.741	235.850	0.47	143.390	154.100	6.9
250.000	287.074	286.480	−0.20	201.673	212.380	5.0
298.150	326.468	325.310	−0.35	255.858	266.270	3.9
350.000	359.477	359.030	−0.12	310.957	320.100	3.1
400.000	384.458	385.800	−0.35	360.885	371.000	2.6
500.000	420.031	422.800	0.66	451.162	458.000	1.5
600.000	443.553	443.500	0.44	530.496	545.000	2.7
700.000	460.040	460.700	0.14	600.863	610.000	1.5
800.000	472.288	471.800	−0.10	663.947	669.000	0.70
900.000	482.001	481.000	−0.21	721.200	732.000	1.5
1000.000	490.071	487.750	−0.48	773.591	788.000	1.8
1200.000	502.842	499.700	−0.63	866.97	880.000	1.5
1500.000	519.870	514.500	−1.0	986.0	1000.000	1.3
2000.000	543.200	535.900	−1.4	1154.6		
3000.000	580.300	572.700	−1.3	1445.0		

* Calorimetric values at 350 K and below are from Haselton and Westrum (1980); values above 400 K are from Tequi et al. (1991). Values above 1300 K are extrapolated.

The calculated entropy for pyrope using Equation 4 shown in Figure 3 is consistently 10 J/mol K lower than, but parallel to, the experimental determinations of Haselton and Westrum (1980) and Tequi et al. (1991), which are from 100 to 1300 K. This offset (Table 3) results from the propagation of the difference between theoretical and experimental heat capacities at around 100 K through the integral relating S to C_P.

Grossular

The calculated heat capacity values for grossular (Table 4) show excellent agreement with the measurements on C_P from 50 to 1000 K, lying generally within the experimental uncertainty of ±1% of calorimetric value for synthetic grossular by Haselton and Westrum (1980) and Krupka et al. (1979). A more detailed examination of the

TABLE 4. Thermodynamic properties of grossular

Temperature K	C_P theory J/mol K	C_P expt syn* J/mol K	C_P difference %	C_P expt nat** J/mol K	S theory J/mol K	S expt syn* J/mol K	S difference %	S expt nat** J/mol K
10.000	0.184	0.071	−159.0	0.293	0.084	0.029	−188	0.142
20.000	1.291	0.803	−60.0	0.930	0.486	0.238	−104	0.490
40.000	7.760	8.293	6.4	8.279	2.824	2.473	−14	2.790
60.000	27.965	27.886	−0.25	26.988	9.377	9.167	−2.3	9.310
80.000	58.325	55.789	−4.5	54.590	21.394	20.861	−2.6	20.700
100.000	92.482	87.738	−5.4	86.105	38.012	36.719	−3.5	34.190
150.000	174.985	168.990	−3.5	167.260	91.526	87.860	−4.2	86.640
200.000	242.392	237.070	−2.2	236.190	151.494	146.190	−3.6	141.915
250.000	294.850	291.080	−1.3	290.530	211.545	205.100	−3.1	203.380
298.150	334.018	333.170	−0.2	331.010	267.113	260.120	−7.7	255.087
350.000	366.508	370.330	1.0	363.000	323.404	316.480	−2.2	313.950
400.000	390.776	396.800	1.5	389.670	374.175	366.020	−2.2	360.968
500.000	424.992	429.700	1.1	425.704	465.693	457.340	−1.8	451.682
600.000	447.358	451.600	0.9	449.670	545.806	537.420	−1.6	531.292
700.000	462.920	462.800	−0.03		616.676	608.040	−1.4	601.384
800.000	474.450	469.300	−1.1		680.087	670.870	−1.4	664.115
900.000	483.509	484.000	0.1		737.465	727.390	−1.4	721.099
1000.000	491.043	498.000	−1.4		789.907	778.810	−1.4	772.217
1200.000	503.370				883.244	870.200	−1.5	
1500.000	518.261				1002.835			
2000.000	543.728				1169.253			
3000.000	597.293				1442.366			

* Calorimetric data at 350 K and below are from Haselton and Westrum (1980); data above 350 K is from Krupka et al. (1979).
** Calorimetric data are from Westrum et al. (1979).

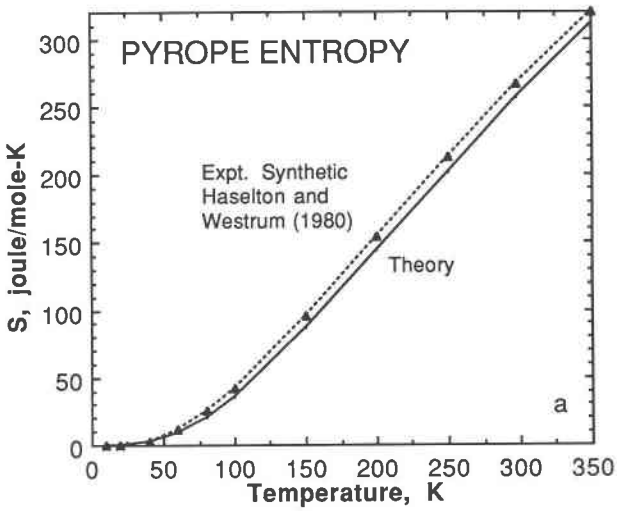

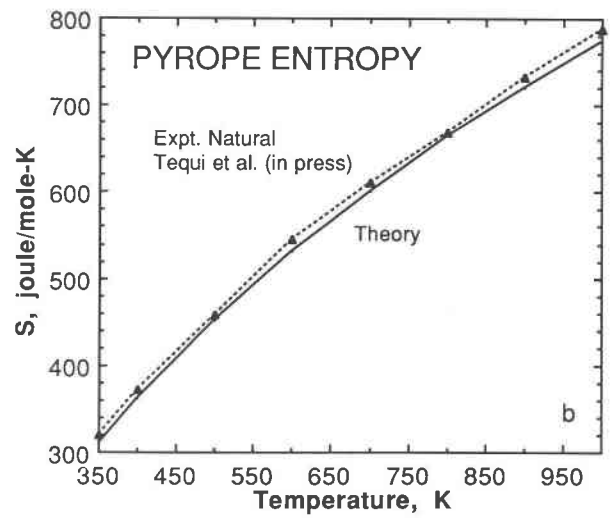

Fig. 3. Entropy of pyrope as a function of temperature. See Figure 2 for explanation.

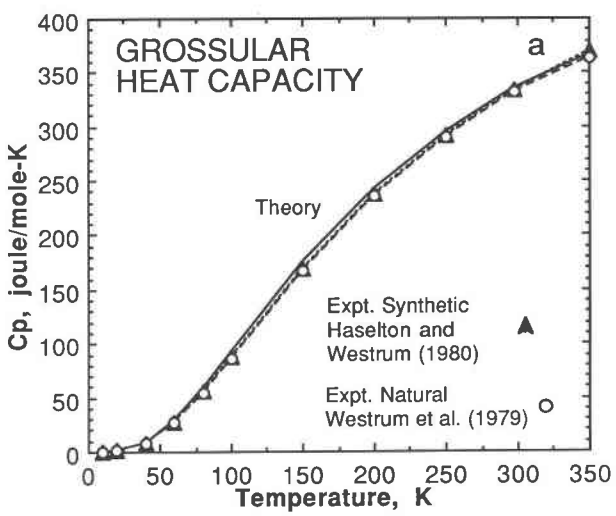

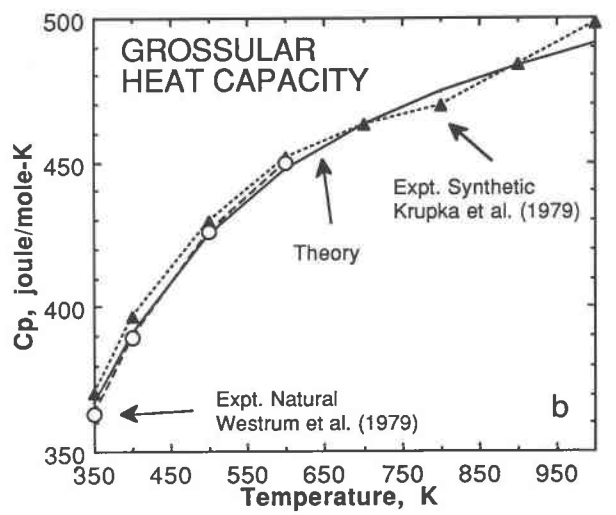

Fig. 4. Heat capacity of grossular as a function of temperature. (**a**) Low temperature expansion. (**b**) High temperature results. (Note different scales for the C_P axis.) Solid line, C_P calculated form Kieffer's model using single-crystal vibrational frequencies measured from natural 98% grossular. Dotted line with filled triangles below 350 K, fit to calorimetric measurements on synthetic grossular by Haselton and Westrum (1980). Dotted line and filled triangles above 350 K are experimental values from Krupka et al. (1979). Dashed line with open circles, calorimetric measureme its on natural grossular by Westrum et al. (1979).

differences between the spectroscopically derived and calorimetrically measured values allows us to evaluate both sets of data.

From 150 to 298 K (Fig. 4a), calculated heat capacity values are slightly higher than, but within the experimental uncertainty of, the calorimetric measurements of synthetic grossular by Haselton and Westrum (1980). (The match from 50 to 150 K is reasonable.) For temperatures greater than 298 K, the calculated values become slightly less than experimental values. Experimental determinations for natural grossular (Westrum et al., 1979) are slightly lower (0.5%) than experimental values on synthetic grossular, so that a crossover point of the calculated values for the synthetic phase with experimental values occurs at a higher temperature of 420 K (Fig. 4b).

High temperature determinations of C_P for synthetic grossular (Krupka et al., 1979) as well as values inferred from natural grossular (Westrum et al., 1979) are equal on average to our calculated values (Fig. 4b) with a maximum difference of 1.5%. From 298 to 700 K, our calculations appear to match the calorimetric data of natural grossular better than those of synthetic grossular. Surprisingly, the largest amount of separation between spectroscopic and calorimetric heat capacities of synthetic grossular occurs at 400–600 K, where calculations based on Kieffer's (1979) model generally yield the best agreement.

Values of calculated entropy for grossular at all tem-

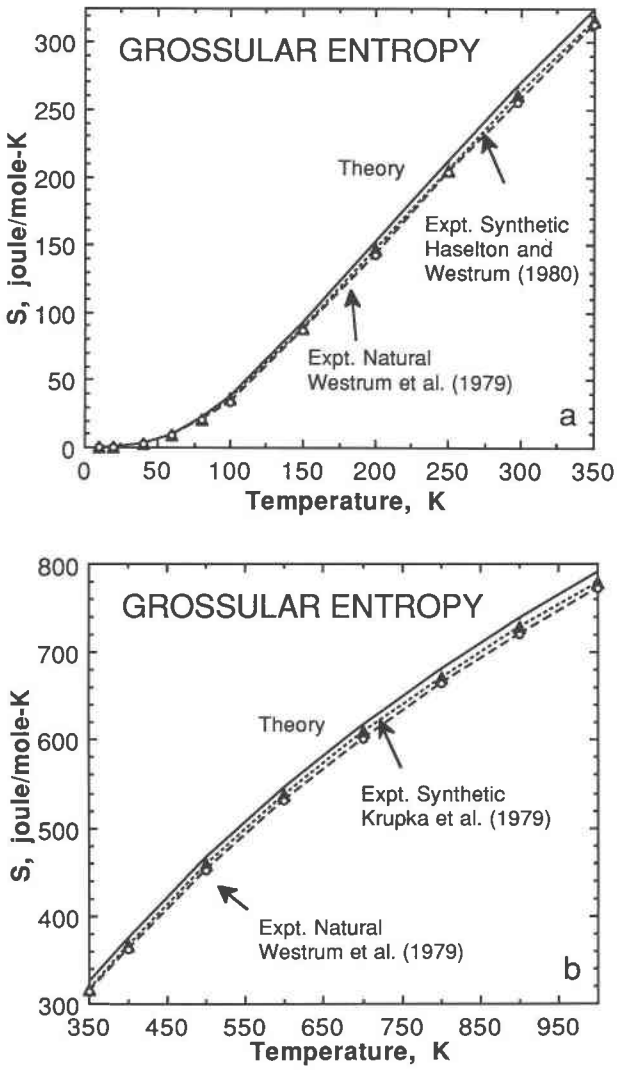

Fig. 5. Entropy of grossular as a function of temperature. See Figure 4 for an explanation of symbols.

peratures above 50 K (Fig. 5) lie a few percent above Haselton and Westrum's (1980) calorimetric entropy values of synthetic grossular, which in turn are consistently a few percent higher than experimental determinations for a natural garnet by Westrum et al. (1979). As occurred for pyrope, the calculated entropy parallels the calorimetric data, indicating simple propagation of the C_P discrepancy between measurements and theory at low temperature.

Assessment of accuracy of calculations and their predictive capabilities

Vibrational modeling of the thermodynamic properties of garnets inherently contains uncertainties because of the approximate nature of the band assignments, the unknown frequencies of the inactive modes, and the existence of dispersion (dependence of frequency on wavevector across the Brillouin zone). The uncertainties caused by these factors are small because the heat capacity is derived from an integral over frequency (Eq. 3), and therefore the model is not particularly sensitive to the exact frequencies of the modes. From Table 1, approximately half of the modes in each category are established and each category covers a narrow range of 50 to 150 cm^{-1}. The presence of a large number of modes over a narrow frequency range, as is certainly the case in garnets, is expected to reduce proportionately the error resulting from ignoring dispersion and estimating unknown inactive modes. As previously mentioned, the existence of a large number of modes for a mineral suggests that its dispersion will be small. The error caused by unknown inactive modes is also low for orthosilicates, such as garnet, in that factor group analysis appears to represent adequately the nature of their vibrations because of strong bonding within the SiO_4 tetrahedron (Hofmeister, 1987; Hofmeister and Chopelas, 1991), and, thus, gives us a reasonable method for approximating inactive modes.

For garnets in particular, the band assignments appear to be a good representation of the actual motions. Internal stretching and bending motions of the Si tetrahedra are clearly distinguished based on the energies of the modes and the existence of distinct trends with X-O bond length or lattice parameter for each type of atomic motion. Similarly, bands connected with Al translations are distinct because these motions are active only in the IR. Assignments of some of the SiO_4 rotations (but not A_g) could be contested, but because these are located in the middle of the other optic continua (Fig. 1), erroneous assignments or the presence of mode mixing with other types of atomic motion will negligibly affect our calculations. Assignments of translations of the dodecahedral cation and of the SiO_4 tetrahedron have little uncertainty because of differences in behavior in solid solution series (Hofmeister and Chopelas, 1991). Moreover, their overlapping and similar energy ranges (Fig. 1) will compensate for any possible errors.

Changing one frequency input by 50 cm^{-1} (that of the Al translations from 477 to 530 cm^{-1}) causes about a 1% increase in C_P near 500 K and smaller decreases at low and high temperatures. This is an upper limit of the uncertainty in our calculations because raising one band through a change in the band assignments will cause another to be lowered.

In summary, we estimate that the uncertainties in heat capacity calculated from spectroscopy are less than 0.5% (i.e., the average difference between theory and calorimetric data for pyrope) for temperatures from 150 to 1300 K. Above 1300 K, uncertainties will be larger because of errors in the anharmonic correction (Eq. 1), and intrinsic anharmonic properties, i.e., contributions of overtones and combinations to the density of states. From 300 to 700 K, the model is expected to achieve its highest accuracy with uncertainties ~0.25%; because anharmonic corrections (Eq. 1) are small and well established, contributions from low and high frequency modes are small,

and the contribution from middle energy modes is well constrained by a high density of modes over a small interval. Below 150 K, the accuracy of the model is probably a few percent because of the possibility that inactive modes could be below the frequency of the lowest lying infrared or Raman mode, or because the low-frequency acoustic modes are not well represented by Debye oscillators. Entropy is calculated within a few percent above 100 K. The larger uncertainty is caused by the propagation of the mismatch in S at low temperature. If S at 298 K is well established, then using this value in conjunction with spectroscopic calculations would result in very accurate values for higher temperature entropy (<0.5% uncertainty).

We infer that C_P and S of majorite could be estimated within a few percent from the incomplete spectroscopic data available now. If the complete single-crystal spectra are established, the lattice contribution to the thermodynamic properties of $MgSiO_3$ garnet, or any other garnet for that matter, can be predicted to better than 0.5% based on our model density of states. We suggest that a similar degree of accuracy can be attained for any other orthosilicate. For other classes of minerals, the degree of accuracy will depend on the precision with which the inactive modes can be predicted, and the appropriateness of the mode assignments. Thermodynamic properties are likely to be predictable for structures that have a large number of modes or a small proportion of inactive modes, given that the measured vibrational spectra are accurate and complete.

Discussion of the excess entropy of pyrope

The calorimetric entropy of pyrope exceeds that of grossular, contrary to expectations. We can now independently evaluate the measurements by comparing spectroscopically derived entropies for pyrope and grossular and by considering their underlying causes. As discussed in the previous sections, the calculations must give the correct relative entropies because their differences exceed the largest possible uncertainties for this method. This conclusion is supported by the correct prediction of bulk moduli of garnets relative to each other from the same assignments for vibrational frequencies (Hofmeister, in preparation).

From Figure 6, it is obvious that the theoretical entropy of pyrope is less than that of grossular for all temperatures, the difference decreasing asymptotically to −16 J/mol K at 800 K. This trend is opposite to that of the experimental entropies wherein that of pyrope exceeds that of grossular at all temperatures except near 500 or 800 K. Note that the experimental value of S for grossular is greater than the theoretical value for pyrope, and the theoretical value of S for grossular is greater than the experimental value for pyrope. Thus, chemical or structural variations occurring with either garnet (discussed below) could account for the excess entropy of pyrope, although the existence of problems with both data sets cannot be ruled out.

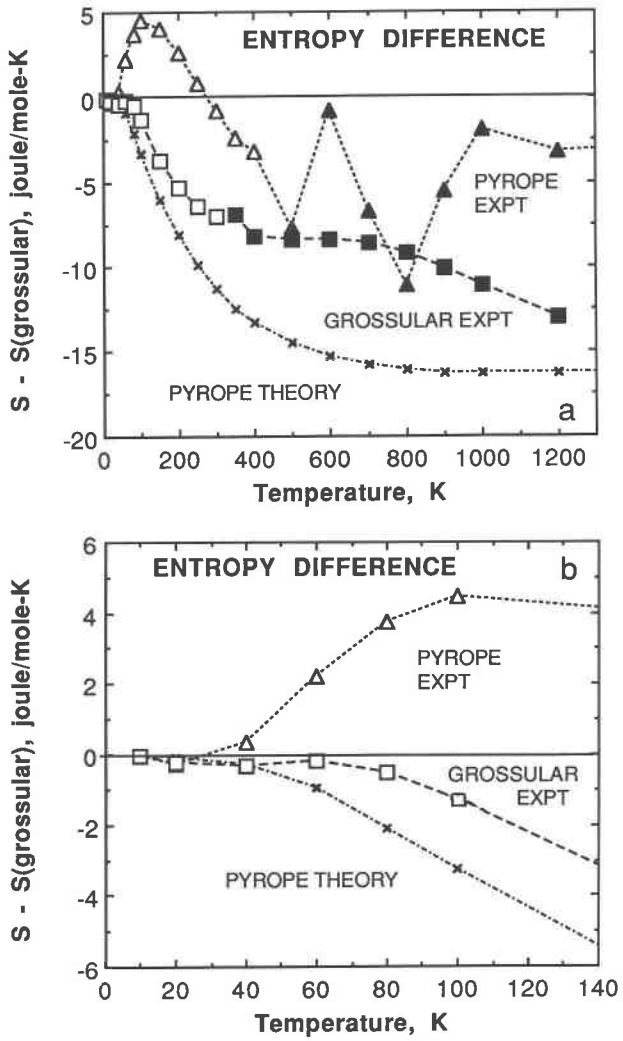

Fig. 6. Comparison of pyrope and grossular entropies by difference. (**a**) High temperatures. (**b**) Low temperature expansion. The calculated entropy of synthetic grossular was chosen as the reference and is shown as the solid line at zero. Dashed line with open squares, experimental measurements of Haselton and Westrum (1980) for synthetic grossular; filled squares are data of Krupka et al. (1979). Dash-dotted line with X's, theory for pyrope. Long dashed line with open triangles, experimental data on synthetic pyrope of Haselton and Westrum (1980); filled triangles are data on natural, nearly pure pyrope from Tequi et al. (1991).

Previous estimates of the entropies of pyrope and grossular from volume-based schemes and oxide summations (Saxena, 1976; Cantor, 1977) have indicated that the entropy of grossular should be about 40 J/mol K higher than that of pyrope at 298 K. Our results indicate the difference should be much smaller (11 J/mol K) but in the same direction.

The microscopic basis for grossular possessing only slightly more entropy than pyrope at low temperatures can be deduced from the distribution of modes over fre-

quency. Figure 1 shows that the density of modes in the optic continua of pyrope and grossular are remarkedly similar, except for the dodecahedral translations and the stretching motions of the Si tetrahedra. As expected, translations of Ca are at lower energies, but surprisingly are not significantly reduced. The nearly identical ranges for the low-lying SiO_4 translations and the acoustic modes constrain the low temperature heat capacities to be very similar. The heat capacity of grossular is only slightly larger by around 200 K because of the slight downward shift in Ca translation frequencies relative to those of Mg, and a compensatory slight upward shift in the frequencies of the SiO_4 translations. As temperature is increased, this difference is undisturbed because the next lowest groups of modes (rotations and Al translations) occupy the same frequency ranges. At moderate to high temperatures, the lower frequency of SiO_4 bending and stretching motions in grossular will contribute to its heat capacity at lower temperatures, causing the grossular entropy to increase relative to that of pyrope until very high temperatures are reached. Thus, based on its overall lower frequencies, which are related to larger cation mass and lattice parameter (Hofmeister and Chopelas, 1991), grossular should have a higher entropy. The magnitude is limited by the closeness of the translational energies of SiO_4, which is determined by the difference in bonding of Si-O in the two garnets. For pyrope, the Si-O bond length of 1.628 Å (Novak and Gibbs, 1971) is typical of silicates and its translational energies are small. For grossular, the large Ca ion forces the tetrahedra to stretch through edge sharing with the larger Ca dodecahedron creating an atypically large Si-O bond length (1.643 Å; Novak and Gibbs 1971). Thus, Si-O and X-O relative bond strengths in grossular differ considerably from those in pyralspites, which in turn alters the force constants for the SiO_4 translations (see Hofmeister and Chopelas, 1991 for further discussion). This effect is not present in other Ca-bearing silicates because dilation of the pyroxene, amphibole, or olivine structures to accommodate the large Ca ion occurs without affecting tetrahedral bond lengths.

The difference in Si-O bonding as controlled by the size of the dodecahedral cation is also the fundamental reason for the existence of the two essentially separate garnet ternaries (pyralspite and ugrandite) and the variation and nonideality in mixing properties among the various binaries. The microscopic basis for compositional dependence in volume properties is discussed by Hofmeister and Chopelas (1991). Quantitative evaluation of entropy of mixing can now be made once accurate and complete vibrational spectra are available on intermediates.

Preferred representation for thermodynamic data

Pyrope

Heat capacities calculated from spectra of natural pyrope closely match calorimetric measurements over a wide temperature range (150–1300 K; see Fig. 2). From about 50 to 150 K, measured heat capacity is significantly in excess of the theory. This, coupled with the nearly constant offset in theoretical from experimental entropy from 100 to 800 K, and the higher experimental value of S relative to grossular leads us to propose that the calorimetric data could incorrectly represent pyrope heat capacities and entropies at low temperature. At least one of the calorimetric data sets does not represent that of the ideal end-member garnet, because if both were correct, the theory would consistently either overestimate or underestimate the values for heat capacity for both garnets. Instead, the measured C_P value of pyrope is above the calculated theoretical value, whereas that of grossular is below. For entropy, this difference is propagated to high temperature. For pyrope, the additional calorimetric entropy could arise from Mg being partially positionally disordered in the synthetic pyrope used for calorimetry by Haselton and Westrum (1980). First, the additional entropy appears at very low temperatures, indicating the ease with which the disorder occurs, as would be expected. Second, the entropy change is smaller than the amount calculated for complete disorder on a per mole basis from statistical thermodynamics by

$$S_{\text{position}} = -\mathrm{R}\,\frac{\mathrm{m}}{Z}\sum P_i \ln P_i \qquad (5)$$

where P_i is the probability of finding Mg^{2+} at the ith position at the dodecahedral site, m is the site multiplicity, Z is the number of formulas per cell, and R is the gas constant (Ulbrich and Waldbaum, 1976). Consideration of the geometry of the dodecahedron suggests that there could be four places for the small Mg ion. (One can also view the positional disorder as the one site having four possible distortions, but it is not correct to describe the dodecahedron as four sites with one full and three empty.) Because there are 24 equivalent Mg sites in the unit cell with a possibility of four positions each, Equation 5 gives S_{position} as 34.5 J/mol K. This value is much larger than the discrepancy of 10 J/mol K that we observed between the spectroscopically and calorimetrically derived entropies, and may indicate that partial positional disorder occurs with approximately 25% of the Mg ions being affected. Alternatively, it is possible that there are two, three, or more than four places for Mg in the scalene dodecahedra. In all cases, S_{position} is larger than observed. Similar behavior, where calculated entropy of configurational disorder is larger than experiment, has been observed in $MgAl_2O_4$ by Wood et al. (1986).

The positional disorder may either result from formation conditions (synthetic phases are quenched from crystallization temperatures of 1637 K) or be inherent in the pyrope structure as a consequence of the large dodecahedral site created by the AlO_6-SiO_4 network. These possibilities would be distinguished through low-temperature calorimetry of pure natural pyrope (e.g., Dora Maira: Chopin, 1984).

In the Raman spectrum of natural pyrope (Hofmeister and Chopelas, 1991), a very low frequency mode at 145

cm^{-1} was observed, but was clearly not a fundamental. This mode may result from the inferred positional disorder, which would lower the site symmetry and allow a new mode. Inclusion of the 145 cm^{-1} band in the density of states of pyrope would produce an additional calculated contribution to entropy that is equal to that observed by calorimetry. This could be tested by Raman spectra of pyrope at low temperature or high pressure and on intermediate compositions of the Py-Gr binary system.

Thermodynamic properties for pyrope at 298.15 K, excluding $S_{position}$, are 326 ± 0.5 J/mol K for C_P and 256 ± 1 J/mol K for S-S_o. The latter value exactly equals the oxide summation value of Saxena (1976) and is within the uncertainty of S inferred from equilibrium relations by Lane and Ganguly (1979).

Grossular

The very good agreement between the calculated thermodynamic properties of the natural grossular and the calorimetric measurements of the synthetic grossular suggests that the values for synthetic grossular of Haselton and Westrum (1980) and Krupka et al. (1979) are likely the best representation of the thermodynamic parameters. We note, however, that the greatest discrepancies in the heat capacities occur where the model is most accurate (400–600 K). The experimental values of C_P are less than theoretical values for temperatures less than 300 K, but are greater when T exceeds 300 K.

One source of the discrepancy between calculations and experiment could result from the presence of a hydrogrossular component in the synthetic sample. Preparation of a gell of the synthetic sample measured by Krupka et al. (1979) is highly likely to give rise to H_2O impurities in the sample. The total weight percent for microprobe analyses of synthetic grossular used by Haselton and Westrum (1980) was low, suggesting that H_2O is present. Translations of the tetrahedron occur at the lowest frequencies observed, so that the calculated thermodynamic properties depend on the constituents of the tetrahedron. H impurities are light, so that their presence would increase the frequency of the lowest lying bands. Thus, garnets containing hydrogrossular would have lower heat capacity than pure grossular at low temperature and higher heat capacities at higher temperature, which is the same as the relation between calculated and measured C_P. Discussion cannot be quantified until vibrational data are available for hydrogrossular.

The natural sample used for calorimetry by Westrum et al. (1979) is from Asbestos, Quebec. Grossular from this locality is birefringent, possesses OH, and has lowered symmetry (Allen and Buseck, 1988). The presence of 5% almandine and spessartine components were estimated to raise the heat capacity of the sample by about 0.5%. Because the calorimetric results for synthetic end-member grossular give low-temperature heat capacities mostly within 1% of C_P for the natural sample containing obvious sources of error, the data from the synthetic material may also be problematic.

For grossular, thermodynamic properties at 298.15 K, excluding nonideal behavior, should be 333.5 ± 0.5 J/mol K for C_P and 265 ± 2 J/mol K for S-S_o. The entropy is considerably less than that for the oxide summation value of 294 J/mol K (Saxena, 1976) but is consistent with entropies of formation derived from various reactions (Newton, 1987) if a small configurational entropy exists for anorthite. That our proposed values differ from calorimetric results both for the synthetic sample by Haselton and Westrum (1980) and on a natural sample by Westrum et al. (1979) may explain the lack of consensus as to which value is better (e.g., Haas et al., 1981; Berman et al., 1985; Halbach and Chatterjee, 1984; Holland and Powell, 1985; Wood and Holloway, 1984).

We suggest that, in lieu of calorimetric measurements on pure grossular, the values derived from spectroscopy could be used as an accurate representation for grossular.

Petrologic implications

Koziol and Newton (1988) prefer the C_P data for synthetic grossular based on configurational entropy for anorthite derived from this quantity and their determination of the anorthite breakdown reaction. Our results support their contention. Use of our values for grossular at 1000 K would slightly increase the configurational entropy for anorthite to essentially 6 ± 4 J/K. This value corresponds to 3–15% tetrahedral Al-Si disorder. An indeterminant amount of disorder has been observed through X-ray diffraction of anorthite at high temperatures (Smith, 1974).

Use of previous thermodynamic properties for pyrope and the reaction boundary (2 enstatite + spinel = forsterite + pyrope) results in an excessively high configurational entropy for $MgAl_2O_4$ (Wood et al., 1986). Use of our lower value for the entropy of pyrope would reduce the predicted values by the appropriate amount (~9 J/mol K), eliminating the need for S_{config} for spinel.

Use of our entropy for pyrope in Newton's (1987) derivation of the enthalpy of formation from reaction of pyrope to form enstatite and corundum gives $\Delta H_{f,298.15}$ of −77.3 ± 2.5 kJ, which is within the experimental uncertainty of that found by Charlu et al. (1975) by drop calorimetry. Thus, our value for entropy of pyrope is consistent with thermodynamic properties of enstatite, spinel, and corundum.

Summary and conclusions

Heat capacity C_V and entropy are calculated for pure pyrope and grossular from complete single-crystal infrared and Raman spectra obtained using natural, nearly end-member garnets (Hofmeister and Chopelas, 1991) using a modified Kieffer-type model. The density of states used in the thermodynamic calculations was constrained from factor group analysis and band assignments based on chemical substitution. Our results match C_P for synthetic and natural pyrope within 0.5% from ~150 to ~1000 K. For grossular, the difference is 1%. The entropy of pyrope is offset by about −10 J/mol K because of

propagation of C_P mismatch at low temperatures. For grossular, calculated S is offset from experiment by +8 J/mol K. Our calculations indicate that the entropy of pyrope should be less than that of grossular for all temperatures. The values of S from spectroscopy are consistent with entropies of formation derived from various reactions, if anorthite possesses configurational entropy due to Al-Si disorder. We propose that either the synthetic pyrope used had Mg positional disorder, leading to excess entropy at low temperatures, or the synthetic grossular had a small amount of 4H substituting for Si, leading to reduced entropy at low temperatures. Whether this disorder is inherent in all pyrope because of the large size of the Mg site compared to the ionic radius, or whether it is dependent on formation conditions can be tested through spectroscopic study of intermediate solid solutions.

Sufficient accuracy has now been attained in spectroscopic derivations of thermodynamic properties of garnets that these calculations can be used predictively, as well as to evaluate the calorimetric measurements. This conclusion is applicable to all orthosilicates, with the obvious stipulation that the measured vibrational spectrum must be complete and correct. Extrapolation can be made with confidence to other minerals, provided that their inactive modes can either be predicted from existing vibrational data or that their number is proportionately small.

Acknowledgments

We thank P. Richet and C. Tequi (Institut de Physique du Globe de Paris) for sharing data with us in advance of publication. Critical comments from R. Burns (Massachusetts Institute of Technology), C.W. Burnham (Harvard), and an anonymous reviewer led to substantial improvements in the manuscript. Support for this project was provided by NSF grant EAR-8816531 and a Fellowship in Science and Engineering from the David and Lucile Packard Foundation.

References cited

Allen, F.M., and Buseck, P.R. (1988) XRD, FTIR, and TEM studies of optically anisotropic grossular garnets. American Mineralogist, 73, 568–584.

Bass, J.D. (1989) Elasticity of grossular and spessartite garnets by Brillouin spectroscopy. Journal of Geophysical Research, 94, 7621–7628.

Berman, R.G. (1990) Mixing properties of Ca-Mg-Fe-Mn garnets. American Mineralogist, 75, 328–344.

Berman, R.G., Brown, T.H., and Greenwood, H.J. (1985) An internally consistent thermodynamic database for mineral in the system Na_2O-K_2O-CaO-MgO-FeO-Al_2O_3-SiO_2-TiO_2-H_2O-CO_2. Document no. TR-377, Scientific Document Distribution Office, Atomic Energy of Canada Limited, Research Company, Chalk River, Ontario, Canada.

Cantor, S. (1977) Entropy estimates of garnets and other silicates. Science, 198, 206–207.

Charlu, T.V., Newton, R.C., and Kleppa, O.J. (1975) Enthalpies of formation at 970 K of compounds in the system MgO-Al_2O_3-SiO_2 by high temperature solution calorimetry. Geochimica et Cosmochimica Acta, 39, 1487–1497.

Chopelas, A. (1990) Thermal properties of forsterite at mantle pressures derived from vibrational spectroscopy. Physics and Chemistry of Minerals, 17, 249–257.

Chopin, C. (1984) Coesite and pure pyrope in high-grade blueschists of the Western Alps: A first record and some consequences. Contributions to Mineralogy and Petrology, 86, 107–118.

Farmer, V.C., and Lazarev, A.N. (1974) Symmetry and crystal vibrations. In V.C. Farmer, Ed., The infrared spectra of minerals, p. 51–68. Mineralogical Society, London.

Fateley, W.G., McDevitt, N.T., and Bently, F.F. (1971) Infrared and Raman selection rules for lattice vibrations: The correlation method. Applied Spectroscopy, 25, 155–174.

Hass, J.L., Robinson, G.R., and Hemingway, B.S. (1981) Thermodynamic tabulations for selected phases in the system CaO-Al_2O_3-SiO_2-H_2O at 101.325 kP (1 atm) between 273.15 and 1,800 K. Journal of Physical Chemistry Reference Data, 10, 575–669.

Halbach, H., and Chatterjee, N.D. (1984) An internally consistent set of thermodynamic data for twenty-one CaO-Al_2O_3-SiO_2-H_2O phases by linear parametric programming. Contributions to Mineralogy and Petrology, 88, 14–23.

Haselton, H.T., Jr., and Westrum, E.F., Jr. (1980) Low-temperature heat capacities of synthetic pyrope, grossular, and $pyrope_{60}grossular_{40}$. Geochimica et Cosmochimica Acta, 701–709.

Hodges, K.V., and McKenna, L.W. (1987) Realistic propagation of uncertainties in geologic thermobarometry. American Mineralogist, 70, 671–709.

Hofmeister, A.M. (1987) Single-crystal absorption and reflection infrared spectroscopy of forsterite and fayalite. Physics and Chemistry of Minerals, 14, 499–513.

Hofmeister, A.M., and Chopelas, A. (1991) Vibrational spectroscopy of endmember silicate garnets. Physics and Chemistry of Minerals, in press.

Hofmeister, A.M., Hoering, T.C., and Virgo, D. (1987) Vibrational spectra of beryllium aluminosilicates: Heat capacity calculations. Physics and Chemistry of Minerals, 14, 205–224.

Holland, T.J.B., and Powell, R. (1985) An internally consistent thermodynamic data set with uncertainties and correlation: 2. Data and results. Metamorphic Petrology, 3, 343–353.

Kieffer, S.W. (1979) Thermodynamics and lattice vibrations of mineral: 3. Lattice dynamics and an approximation for minerals with application to simple substances and framework silicates. Reviews of Geophysics and Space Physics, 17, 35–39.

——— (1980) Thermodynamics and lattice vibrations of minerals: 4. Application to chain and sheet silicates and orthosilicates. Reviews of Geophysics and Space Physics, 18, 862–886.

Kolesnik, Y.N., Nogteva, V.V., Arkhipendo, D.K., Oreknov, A.A., and Paukov, I.Y. (1979) Thermodynamics of pyrope-grossular solid solution and the specific heat of grossular at 13–300 K. Geochemistry International, 16, 57–64.

Koziol, A.M., and Newton, R.C. (1988) Redetermination of the anorthite breakdown reaction and improvement of the plagioclase-garnet-Al_2SiO_5-quartz geobarometer. American Mineralogist, 73, 216–223.

Krupka, K.M., Robie, R.A., and Hemingway, B.S. (1979) High-temperature heat capacities of corundum, periclase, anorthite, $CaAl_2Si_2O_8$ glass, muscovite, pyrophyllite, $KAlSi_3O_8$ glass, grossular, and $NaAlSi_3O_8$ glass. American Mineralogist, 64, 86–101.

Lane, D.L., and Ganguly, J. (1979) Reevaluation of Al_2O_3 solubility in orthopyroxene in the garnet and spinel fields, and the entropy of pyrope. Geological Society of America Abstracts with Programs, 11, 462.

Newton, R.C. (1987) Thermodynamic analysis of phase equilibria in simple mineral systems. In Mineralogical Society of America Reviews in Mineralogy, 17, 1–34.

Newton, R.C., and Wood, B.J. (1980) Volume behavior of silicate solid solutions. American Mineralogist, 65, 733–745.

Novak, G.A., and Gibbs, G.V. (1971) The crystal chemistry of the silicate garnets. American Mineralogist, 56, 791–825.

O'Neill, B., Bass, J., Smyth, J.R., and Vaughan, M.T. (1989) Elasticity of a grossular-pyrope-almandine garnet. Journal of Geophysical Research, 94, 17819–17824.

Reif, F. (1965) Fundamentals of statistical and thermal physics. McGraw-Hill, New York.

Saxena, S.K. (1976) Entropy estimates for some silicates at 298 K from molar volumes. Science, 193, 1241–1242.

Skinner, B.J. (1966) Thermal expansion. In S.P. Clark, Jr., Ed., Handbook of physical constants, Memoir 97, p. 75–96. Geological Society of America, Boulder, Colorado.

Smith, J.V. (1974) Feldspar minerals, vol. I. Crystal structure and physical properties. Springer-Verlag, New York.

Sumino, Y., and Anderson, O.L. (1984) Elastic constants of minerals. In S. Carmichael, Ed., CRC handbook of the physical properties of rocks, p. 139–280. CRC Press, Boca Raton, Florida.

Tequi, C., Robie, R.A., Hemingway, B.S., Neuville, D., and Richet, P. (1991) Thermodynamic and melting properties of pyrope. Geochimica et Cosmochimica Acta, in press.

Ulbrich, H.H., and Waldbaum, D.R. (1976) Structural and other contributions to the third-law entropies of silicates. Geochimica et Cosmochimica Acta, 40, 1–24.

Watanabe, J. (1982) Thermochemical properties of synthetic high-pressure compounds relevant to the Earth's mantle. In S. Akinoto and M.H. Manghnani, Eds., High pressure research in geophysics, p. 441–464. Center for Academic Publications, Tokyo.

Westrum, E.F., Jr., Essene, E.J., and Perkins, D., III (1979) Thermophysical properties of the garnet, grossular: $Ca_3Al_2Si_3O_{12}$. Journal of Chemical Thermodynamics, 11, 57–66.

Wood, B.J., and Holloway, J.R. (1984) A thermodynamic model for subsolidus equilibria in the system CaO-MgO-Al_2O_3-SiO_2. Geochimica et Cosmochimica Acta, 48, 159–176.

Wood, B.J., Kirkpatrick, R.J., and Montez, B. (1986) Order-disorder in $MgAl_2O_4$ spinel. American Mineralogist, 71, 999–1008.

Manuscript received January 31, 1990
Manuscript accepted February 21, 1991